Near-critical confined fluids and Ising films: Density-matrix renormalization-group study

A. Maciołek,[1] A. Drzewiński,[2] and R. Evans[3]
[1]*Institute of Physical Chemistry, Polish Academy of Sciences, Department III, Kasprzaka 44/52, PL-01-224 Warsaw, Poland*
[2]*Institute of Low Temperature and Structure Research, Polish Academy of Sciences, P.O. Box 1410, Wrocław 2, Poland*
[3]*H.H. Wills Physics Laboratory, University of Bristol, Bristol BS8 1TL, United Kingdom*
(Received 5 July 2001; published 30 October 2001)

Two-dimensional Ising strips subject to identical surface fields $h_1=h_2\geqslant 0$ are studied for temperatures above and below the bulk critical temperature T_c and a range of bulk fields h by means of the density-matrix renormalization-group method. In the case of nonvanishing surface fields, the near-critical behavior of the solvation force f_{solv}, total adsorption Γ, inverse longitudinal correlation length $\xi_{\parallel}^{-1}$ and specific heat C_H is strongly influenced by the (pseudo) capillary condensation that occurs below T_c. We obtain scaling functions of f_{solv}, Γ, and $\xi_{\parallel}^{-1}$. C_H exhibits a weakly rounded singularity on crossing the pseudocoexistence line. We contrast these results with those for the case of free boundaries where, for temperatures slightly below T_c, f_{solv} and C_H exhibit a sharp extremum away from $h=0$. Our results have direct repercussions for the properties of near-critical Ising films in three dimensions and we argue that the long-ranged solvation (Casimir) force in confined fluids should be more attractive in the neighborhood of the capillary critical point than exactly at the bulk critical point.

DOI: 10.1103/PhysRevE.64.056137 PACS number(s): 05.70.Jk, 64.60.Fr, 68.35.Rh, 68.15.+e

I. INTRODUCTION

When simple fluids are confined between parallel substrates or walls their properties may differ dramatically from those in bulk. Understanding the influence of confinement on the phase behavior of the fluid is relevant for fluids in porous solids and for experiments performed with the surface force apparatus [1,2]. The properties of the confined fluid near bulk criticality are particularly rich since the combined effects of finite-size and specific wall-fluid interactions have a profound effect on critical behavior. Scaling analysis implies that finite-size effects will shift the critical temperature and, depending on boundary conditions, lead to rounding of critical singularities [3,4]. Surface effects may induce a shift in the critical chemical potential μ [5] and introduce nonuniformity of the local order parameter which entails surface critical exponents; the theory of surface critical phenomena predicts fundamentally different universality classes depending on the type of surface [5–7]. One of the challenges for the theory of confined fluids near bulk criticality is to understand the interplay between the various phenomena that arise in the critical region and this is the subject of the present paper.

When the confining walls attract the atoms of the fluid, the phenomenon of capillary condensation [1,2] occurs at temperatures T below the bulk critical temperature T_c whereby the bulk first-order phase transition is displaced in the (T,μ) plane: condensation of the gas to liquid occurs at a value of μ smaller than in bulk. On the other hand, at the bulk critical point, the critical Casimir effect arises [8]. Finite-size contributions to the free energy of a fluid confined between two parallel walls, separated by a distance L, give rise to a force per unit area between the walls, or an excess pressure, termed the solvation force f_{solv} [1]. The detailed form of f_{solv} depends on the bulk state point and the wall-fluid potentials, as well as on L. At the critical point, f_{solv} becomes long ranged as a result of critical fluctuations [9], a phenomenon that is analogous to the well-known Casimir effect in electromagnetism [10]. Here, we are concerned with properties of the confined fluid and, in particular, the solvation force for temperatures between the bulk critical temperature T_c and the shifted or capillary critical temperature $T_{cL}(<T_c)$ which denotes the end of the capillary condensation line. For large L, the two different critical points are located close to each other in the (T,μ) plane and we find capillary condensation has a very strong influence on the near-critical solvation (Casimir) force and on other thermodynamic properties.

Treated separately, the two phenomena have received much attention. The theory of capillary condensation is well developed [1,5,11,12] and the predicted behavior of f_{solv}, which jumps discontinuously, and other quantities at this transition has been confirmed in computer simulations and in experiments [1,2]. The critical Casimir effect has attracted much recent interest due to the universal character of this phenomenon. The existence of the long-ranged critical Casimir force should be common to all systems characterized by fluctuating quantities with external constraints [8]. Although unambiguous experimental verification of the effect is beset with difficulties [8,13], some recent experiments do provide evidence for its existence [14]. One of the sources of experimental difficulty is that the predicted leading power-law decay of the Casimir force at bulk criticality, $f_{solv}(L) \sim k_B T_c A_{12}(d-1)L^{-d}$ as $L\to\infty$, is for (bulk) spatial dimension $d=3$, of the same form as the solvation force arising from dispersion forces and for many experimental situations the amplitude may be much smaller than the corresponding Hamaker constant [8,15]. Considerable effort has been spent in calculating the values of the Casimir amplitude A_{12} for different boundary conditions [8,15]. A_{12} is a universal number for $2\leqslant d\leqslant d_>$, where the upper critical dimension $d_>=4$ for the Ising universality class. The value of A_{12} depends on the type of boundary conditions imposed on the two walls: 1 refers to $z=1$ and 2 to $z=L$. For experiments on pure fluids or binary mixtures, the most relevant situation is

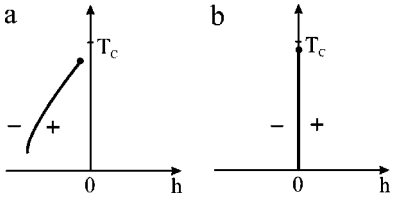

FIG. 1. Schematic temperature—bulk magnetic field (T,h) phase diagrams for an Ising system subject to identical surface fields $h_1=h_2$ and a fixed (large) surface separation L. In (a) $h_1=h_2\gg 0$ and capillary condensation of the $(+)$ spin-up phase occurs along the solid line $h_{co}(T)<0$. This line ends in the capillary critical point (T_{cL},h_{cL}) (circle) with $T_{cL}<T_c$, the bulk critical temperature, and $h_{cL}<0$. In (b), $h_1=h_2=0$ (free boundaries) and the bulk Ising symmetry is preserved, i.e., coexistence occurs along the solid line $h=0$ up to the temperature $T_{cL}<T_c$. In the two-dimensional Ising strip, the coexistence lines become lines of pseudocoexistence, i.e., the first-order transitions are very weakly rounded.

when the walls exert surface fields on the atoms of a fluid, i.e., symmetry-breaking boundary conditions. In the case of identical walls and $d=3$, the Casimir amplitude is estimated to be $A_{11}\equiv A_{++}\sim -0.35$ from Monte Carlo simulations [16], whereas a recent local functional treatment yields a value of -0.428 [17]. Since fluctuations in bulk fluids are of the largest extent exactly at the critical point, one may expect that the effect of the external constraints, such as confining walls, should also be largest exactly at the critical point. However, knowledge of the solvation force slightly away from the the bulk critical point and, in particular, at thermodynamic states lying between the capillary critical point and the bulk critical point is very limited. It is, of course, much more difficult to develop a theory of the crossover regime, since it is not clear *a priori* which degrees of freedom are irrelevant, and it is not obvious which simplifying assumptions can be made. Given that there are no reliable general predictions, it is most valuable to have accurate results for a model system.

Here we exploit the mapping between fluids and the Ising model and consider Ising spin systems subject to identical surface fields $h_1=h_2\geqslant 0$. The bulk magnetic field h corresponds to the chemical-potential difference $\mu-\mu_{sat}$. Schematic phase diagrams are shown in Fig. 1. Mean-field results are available for the temperature dependence of the solvation force at $h=0$ or, equivalently, for the scaling function $\mathcal{W}_{++}$ [16–18], defined by $f_{solv}/k_BT_c\equiv L^{-d}\mathcal{W}_{++}(L/\xi_b)$ where ξ_b is the bulk correlation length. The solvation force has a shallow minimum above T_c that occurs for $L\sim 3.7\xi_b$. Local functional results for $d=3$ from Borjan and Upton [17] yield a more pronounced minimum in W_{++} at $L\sim 3.1\xi_b$. In $d=2$, W_{++} was determined by exact transfer-matrix methods [19]. Once again there is a minimum above T_c, now at $L\sim 2.23\xi_b$, with an amplitude that is 6.6 times the Casimir value $W_{++}(0)=A_{++}(d-1)$.

For $h_1=h_2>0$, the line $h=0$ lies in the liquid or spin up $(+)$ phase away from the line of capillary condensation at $h_{co}(T)$—see Fig. 1(a). Since we are primarily interested in the behavior of f_{solv} in the neighborhood of $h_{co}(T)$ and in the region between the capillary and bulk critical points, we require a technique that is tractable for $h\neq 0$ and for large surface separations L so that we may enter the appropriate scaling regimes. For two-dimensional lattices (strips) the recently developed density-matrix renormalization-group (DMRG) method [20] provides a systematic and very accurate means of calculating the solvation force and other properties in nonvanishing bulk magnetic field h for a wide range of temperatures and for large strip widths L. Results obtained at $T=T_c$ show that f_{solv} has a pronounced minimum at some value $h<0$, which corresponds roughly to the continuation of the capillary condensation line to the critical temperature [21]. The amplitude of the scaling function at the minimum is about 100 times the Casimir value. This observation prompted us to perform a detailed study of the solvation force for several temperatures above and below T_c. We find that a small bulk field $h<0$, which favors gas, or the $(-)$ phase, results in a solvation force that is much more attractive (at the same large value of L) than the Casimir value. We attribute the strong attraction to the residual effects of capillary condensation. This finding has repercussions for experimental studies that aim to measure the Casimir force, e.g., by atomic force microscopy or surface force apparatus. Some of our results were reported in a Letter [22]. The purpose of this paper is to present the results for f_{solv} in more detail by extending the analysis to the scaling behavior and to consider other properties that exhibit features reflecting those found in f_{solv}. We also examine various criteria for determining the coexistence line for capillary condensation. Recall that although there is no longer any true phase transition for finite L, in Ising strips in $d=2$ there is still a line of extremely weakly rounded first-order transitions ending at a pseudocritical point [23–26]. In Ref. [22], we determined the pseudocoexistence line $h_{co}(T)$ and gave an estimate for the pseudocritical temperature T_{cL} on the basis of the behavior of f_{solv}, the adsorption (total magnetization) Γ, and the longitudinal correlation length $\xi_{\|}$. In this paper, we also calculate the specific heat C_H. The form of C_H on crossing the capillary condensation line does not appear to have been investigated previously. We consider paths at: (a) constant temperature, and (b) constant field h, crossing the capillary condensation line. Along both paths, the specific heat develops a (weakly rounded) singularity since the symmetry-breaking surface fields lead to a pseudocoexistence line $h_{co}(T)$ with nonzero slope, and hence, a latent heat that is inversely proportional to L. Finally, we study the case of free boundaries $h_1=h_2=0$ and inquire whether there are any major differences in the behavior of the various properties between this case and $h_1=h_2\gg 0$. As exact results are available along the line of pseudocoexistence $h=0$ [see Fig. 1(b)], these serve as a valuable test for the accuracy of the DMRG method.

Our paper is organized as follows. Section II defines the model and summarizes its phase behavior. Section III describes briefly the DMRG technique and presents our results for strong surface fields. In Sec. IV, we present results for $h_1=h_2=0$. We conclude in Sec. V with a discussion and summary.

II. THE MODEL AND ITS PHASE BEHAVIOR

The system we consider is an Ising spin system in slab geometry subject to identical surface fields. Our DMRG results refer to the $d=2$ Ising strip defined on the square lattice of size $L\times M$, $M\to\infty$. The lattice consists of L parallel rows at spacing $a\equiv 1$, so that the width of the film is $La=L$. At each site, labeled $i,j,\ldots$, there is an Ising spin variable taking the value $\sigma_i=\pm 1$. We assume nearest-neighbor interactions of strength J and a Hamiltonian of the form

$$\mathcal{H}=-J\left[\sum_{\langle i,j\rangle}\sigma_i\sigma_j+h\sum_i\sigma_i+h_1\sum_i^{(1)}\sigma_i+h_2\sum_i^{(L)}\sigma_i\right], \quad (1)$$

where the first sum runs over all nearest-neighbor pairs of sites, while the last two sums run, respectively, over the first and the Lth row. h is the reduced bulk magnetic field and h_1 and h_2 are reduced surface fields corresponding to direct (''contact'') interactions between the surfaces and the spins in the film. We assume that $h_1\equiv h_2\geqslant 0$. The generalization of Eq. (1) to $d=3$ is immediate.

For an Ising film that is of infinite extent in $d-1$ dimensions parallel to the surfaces true two-phase coexistence may occur provided $d-1\geqslant 2$—the lower critical dimension of the corresponding bulk system. Criticality for finite L then lies in the universality class of the bulk $d-1$ system. The location of the critical point in the bulk field, temperature (h,T) plane depends on the choice of surface field:

(a) $h_1=h_2>0$. In this case, the phenomenon equivalent to capillary condensation takes place when the bulk magnetic field $h<0$ favors the negatively magnetized phase, whereas the surface fields h_1,h_2 favor the positively magnetized phase. For large L, two-phase coexistence occurs along a line $h_{co}(T)$ which is given approximately by the analog of the Kelvin equation

$$-h_{co}(T)\approx\sigma(T)/Lm^*(T), \quad (2)$$

where $\sigma(T)$ is the interfacial tension between the coexisting bulk $(+)$ and $(-)$ phases and $m^*(T)>0$ is the bulk spontaneous magnetization. [A brief derivation of Eq. (2) is given in Sec. III.] The presence of thick wetting films of $+$ spin at the two surfaces in the $(-)$ phase gives rise to nontrivial corrections that shift the condensation line to larger values of $|h|$ [1], nevertheless, the Kelvin equation does predict the correct qualitative behavior of the condensation line at low temperatures. The two-phase coexistence ends in a (capillary) critical point (h_{cL},T_{cL}) where $T_{cL}(h_1)$ lies below the temperature of the bulk critical point T_c—see Fig. 1(a). The expression for the critical temperature shift [5] is given by

$$[T_{cL}(h_1)-T_c]/T_c\approx -L^{-1/\nu}X_c(h_1L^{\Delta_1/\nu}), \quad (3)$$

where $X_c(w)$ is a scaling function. A similar form holds for $\Delta h_c\equiv h_{cL}(h_1)$ [5]

$$\Delta h_c\approx -L^{-\Delta/\nu}Y_c(h_1L^{\Delta_1/\nu}), \quad (4)$$

where $Y_c(w)$ is another scaling function. Δ_1 is the surface gap exponent, Δ is the bulk gap exponent, and ν is the bulk correlation length exponent.

(b) $h_1=h_2=0$. In films with free boundaries, the Ising symmetry dictates that two-phase coexistence must be at $h=0$. Thus, for $d\geqslant 3$ and large but finite L, the line of coexistence remains at $h=0$ but ends at the critical temperature $T_{cL}<T_c$ given by Eq. (3) with $X_c(0)=\text{const}$—see Fig. 1(b).

In $d=2$ Ising films. the situation is slightly different. As mentioned earlier, there is no true phase transition for finite L, i.e., no nonanalytic behavior of the free energy. Derivatives of the free energy are rounded, giving rise to extrema rather than singularities. However, the rounding in h or in T is extremely small for large L, namely of the order of $L^{-3/2}\exp[-L\sigma(T)/k_BT]$ [23], so that the *pseudo* first-order transition remains very sharp and may be located by simulation [25] or, indeed, by DMRG [26]. For the $d=2$ Ising model, the surface tension $\sigma(T)$ is given exactly by

$$\sigma(T)=2k_BT(K-K^*), \quad (5)$$

where $K=J/k_BT$ and K^* satisfies $\sinh(2K)\sinh(2K^*)=1$ [27] and the critical exponents are $\nu=1$, $\Delta=15/8$, and $\Delta_1=1/2$ [7]. For sufficiently large L, we expect the scaling results (3) and (4) to remain valid in $d=2$, provided, of course, there is some way of locating the pseudocapillary critical point.

III. DMRG RESULTS FOR STRONG SURFACE FIELDS $h_1=h_2\gg 0$

The DMRG is a technique based on the transfer-matrix approach [20]. It provides an efficient algorithm for constructing the effective transfer matrix for large systems; the effective transfer matrix is then diagonalized numerically. We have used the finite-system version of the DMRG algorithm designed to perform very accurate calculations for finite-size systems [28,29]. As emphasized earlier, the DMRG works equally well for $h\neq 0$, where no exact solutions are available, as for $h=0$ [21,22]. The total free energy f per site is obtained from the largest eigenvalue Λ_0 of the effective transfer matrix

$$\beta f(L,T,h,h_1)=-\frac{1}{L}\ln\Lambda_0, \quad (6)$$

where $\beta=(k_BT)^{-1}$.

A. Solvation force

The total free energy per site of the $d=2$ Ising film with surface fields $h_1=h_2$ may be written as

$$f(L,T,h,h_1)=f_b(T,h)+2f_w(T,h,h_1)/L+f^*(L,T,h,h_1)/L, \quad (7)$$

where f_b is the bulk free energy, f_w is the L-independent surface excess free-energy contribution from each surface, and f^* is the finite-size contribution to the free energy. All energies are measured in units of J and the temperature in

units of J/k_B. f^*, which vanishes for $L\to\infty$, gives rise to the generalized force, which is analogous to the solvation force between the walls in the case of confined fluids [1],

$$f_{solv}=-(\partial f^*/\partial L)_{T,h,h_1}. \tag{8}$$

For Ising systems with identical surface fields, the solvation force is attractive, i.e., $f_{solv}<0$.

From the general theory of critical finite-size scaling [3], it follows that near bulk criticality the solvation force for identical surface fields should take the following scaling form (ignoring nonuniversal metric factors):

$$f_{solv}/k_BT_c=L^{-d}W(L\tau^{\nu},L|h|^{\nu/\Delta},Lh_1^{\nu/\Delta_1}), \tag{9}$$

where W is a universal scaling function, $\tau\equiv(T-T_c)/T_c$, and ν, Δ, and Δ_1 are the critical exponents introduced earlier. As mentioned in the Introduction, at fixed points of the renormalization-group transformation $\tau=0$, $h=0$, $h_1=0$ (or $h_1=\infty$) the leading-order decay of the solvation force for $L\to\infty$ is algebraic since the scaling function reduces to $W(0,0,0)=\mathcal{A}_0(d-1)$ or $W(0,0,\infty)=\mathcal{A}_\infty(d-1)$. $\mathcal{A}_0$ and $\mathcal{A}_\infty$ are the universal Casimir amplitudes. For the $d=2$ Ising model $\mathcal{A}_\infty=\mathcal{A}_0=-\pi/48$ [30].

In order to obtain the solvation force and its scaling functions, we first calculate the excess free energy per unit ''area''

$$f_{ex}(L)\equiv(f-f_b)L. \tag{10}$$

The bulk free energy per spin f_b is known exactly only for $h=0$ [27]. For nonzero bulk field we evaluate f_b numerically. We calculate the largest eigenvalue for finite systems (strips) with free boundary conditions and widths L ranging from 30 to 300. We then extrapolate to $L\to\infty$ using the Bulirsch and Stoer method [31] and obtain the value of f_b for each state point (T,h). Such an extrapolation is guaranteed to be of high accuracy provided the ratio between the width of the largest strip L_{max} and the bulk correlation length ξ_b, is much greater than unity; the smaller L_{max}/ξ_b, the less accurate are the extrapolated values. Special tests were performed at $T=T_c$ where the ratio becomes small [21]. Of course, it is necessary to obtain a very accurate bulk free energy in order to obtain an accurate $f_{ex}(L)$ and, hence, a reliable solvation force. By calculating $f_{ex}(L)$ at L_0+2 and L_0 we obtain $f_{solv}=-\partial f_{ex}(L)/\partial L$ by a finite difference.

Calculations were performed for films of width $L=100$, 150, and 200 at several fixed temperatures above and below T_c. h_1 was chosen separately for each L so that the scaling variable $x\equiv Lh_1^{\nu/\Delta_1}(=Lh_1^2$ in $d=2)=20\,000$, which is sufficient to ensure each system corresponds to the infinite surface field scaling limit [21]. Examples of f_{solv} as a function of h for fixed $L=200$ and various fixed temperatures were given in Fig. 1 of Ref. [22]. Here, in Fig. 2, we plot $L^2f_{solv}/k_BT_c=W(z,y,x)$ as a function of $y\equiv L|h|^{\nu/\Delta}(=L|h|^{8/15}$ in $d=2)$ for fixed $x=20\,000$ and several fixed values of $z\equiv L\tau^{\nu}(=L\tau$ in $d=2)$. For the lowest temperatures considered here, corresponding to the scaling variable z equal to -20 and -10, we find a very weakly rounded jump of the solvation force from zero to a negative value as y is reduced [see Fig. 2(a)]. In the vicinity of the jumps the scaling is not well obeyed. We can understand this by recalling that a discontinous jump is a characteristic signature of the solvation force at a first-order capillary condensation phase transition [1,11]. At fixed large L and fixed temperature $T<T_{cL}$, f_{solv} should change abruptly from values appropriate to a spin down $(-)$ (gas) phase

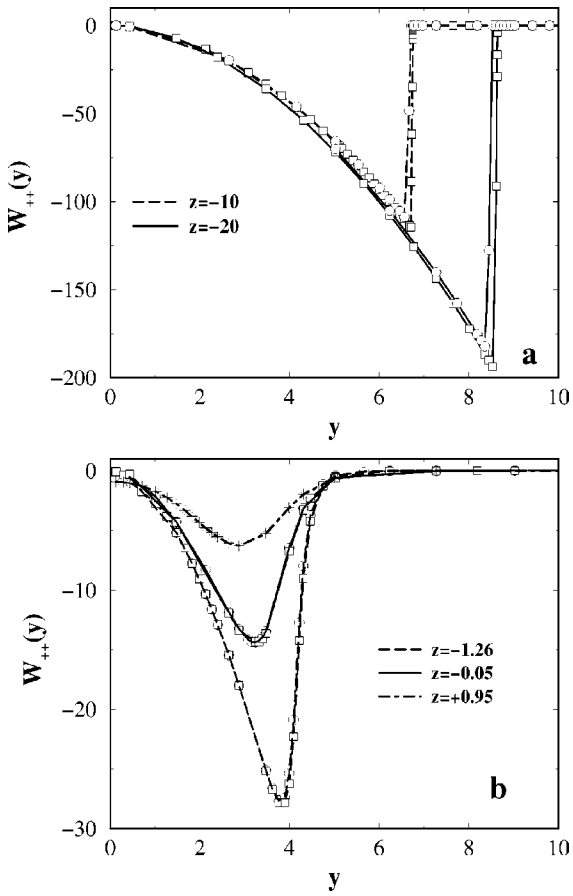

FIG. 2. Dimensionless scaling function of the solvation force $W_{++}(y)\equiv W(z,y,x)=L^2f_{solv}/k_BT_c$ calculated for two-dimensional Ising strips of width $L=70$ (asterisks), 100 (circles), 150 (diamonds), and 200 (squares) plotted as a function of $y=L|h|^{8/15}$ at fixed $x=Lh_1^2=20\,000$ and several choices of the scaling variable $z=L\tau$. In (a) for $z=-20$, -10, the sharp jumps to a strongly attractive solvation force as y is reduced denote capillary condensation of the $(+)$ phase; scaling is not well obeyed. In (b) $z=-1.26$, -0.05, 0.95, the solvation force exhibits a minimum and the scaling is very well obeyed.

$$f_{solv}^{-}\approx 0, \tag{11}$$

to negative values appropriate to a spin up $(+)$ (liquid) phase

$$f_{solv}^{+}\approx[\mu-\mu_{sat}(T)](\rho_l-\rho_g), \tag{12}$$

upon increasing the chemical potential μ [12]. Here, $\mu_{sat}(T)$ is the chemical potential at bulk two-phase coexistence and ρ_l and ρ_g are the coexisting densities of bulk liquid and gas,

respectively. This result is obtained, in magnetic language, from the following (macroscopic) approximation for the total free energy of the two confined phases:

$$f^{\pm} \approx f_b^{\pm}(T,h) + \frac{2}{L} f_w^{\pm}(T,h,h_1), \tag{13}$$

where $\pm$ denotes the two phases and $f_w^{\pm}$ denotes the surface excess free energy for the wall-spin up/down phase. Since this approximation ignores interactions between surfaces, it is valid for $L \to \infty$. We find that in the $(-)$ phase

$$f_{ex}^{-} \approx 2 f_w^{-}(T,h,h_1), \tag{14}$$

which is independent of L so that Eq. (11) follows, while in the $(+)$ phase

$$f_{ex}^{+}(L) \approx L[f_b^{+}(T,h) - f_b^{-}(T,h)] + 2 f_w^{+}(T,h,h_1). \tag{15}$$

Expanding the bulk free energy to first order in h

$$f_b^{\pm}(T,h) \approx f_b^{\pm}(T,0) \mp h m^*(T), \tag{16}$$

where $m^*(T) > 0$ is the bulk spontaneous magnetization, we find

$$f_{ex}^{+}(L) \approx -2Lhm^*(T) + 2 f_w^{+}(T,h,h_1). \tag{17}$$

Recall that for $h < 0$, the $(-)$ phase is stable in bulk so the first term in Eq. (17) reflects the fact that the $(+)$ phase would be metastable in bulk. The resulting solvation force $-\partial f_{ex}(L)/\partial L$ is

$$f_{solv}^{+} \approx 2hm^*(T), \tag{18}$$

which is equivalent to Eq. (12) since $2m^*(T)$ corresponds to $(\rho_l - \rho_g)$ and h to $[\mu - \mu_{sat}(T)]$. The calculated gradients $(\partial f_{solv}^{+}/\partial h)_T$ for $z \leqslant -10$ agree with the known values of $2m^*(T)$ to a relative accuracy 10^{-4} [22].

Coexistence occurs, at $h = h_{co}(T)$, when $f^{+} = f^{-}$. We estimate $h_{co}(T)$ by expanding the surface excess free energies $f_w^{\pm}$ about their values at bulk coexistence $(h = 0)$, i.e., about $\sigma_w^{\pm}(T,h_1)$. To first order in h

$$f_w^{\pm}(T,h,h_1) \approx \sigma_w^{\pm}(T,h_1) - h m_s^{\pm}, \tag{19}$$

where $m_s^{\pm} = -(\partial f_w^{\pm}/\partial h)_{T,h_1}$ is the surface excess magnetization evaluated close to capillary condensation. It follows that

$$-h_{co}(T) \approx \frac{\sigma_w^{-}(T,h_1) - \sigma_w^{+}(T,h_1)}{Lm^*(T) - (m_s^{-} - m_s^{+})}, \tag{20}$$

which is equivalent to results given in Refs. [12,26]. For the strong surface fields h_1 considered here, a single wall is always wet completely by $(+)$ phase so that $\sigma_w^{-}(T,h_1) = \sigma_w^{+}(T,h_1) + \sigma(T)$, where $\sigma(T)$ is the interfacial tension between $(+)$ and $(-)$ phases, and to leading order in $1/L$, Eq. (20) reduces to the Kelvin equation (2). For large L, $|h_{co}(T)|$ is small and thick wetting films of $(+)$ phase develop at the surfaces (walls). Then, $m_s^{-} \approx 2lm^*(T)$, where $l(T,h)$ is the film thickness. By contrast, $m_s^{+} \approx 0$ and Eq. (20) may be rewritten for the complete wetting situation as

$$-h_{co}(T) \approx \frac{\sigma(T)}{m^*(T)[L - 2l(T,h_{co})]}, \tag{21}$$

which is the standard modification to the Kelvin equation, valid for short-ranged forces [1,11]. In $d = 2$ however, fluctuations of the wetting films give rise to an additional contribution to the free energy and $(L - 2l)$ in the denominator of Eq. (21) should be replaced by $(L - 3l)$ [32].

Using the Kelvin equation (2) for $h_{co}(T)$, it follows that the jump in the solvation force is given by

$$\Delta f_{solv} \equiv f_{solv}^{+} - f_{solv}^{-} \approx 2h_{co}(T)m^*(T) \approx -2\sigma(T)/L, \tag{22}$$

i.e., the magnitude of the jump should decrease in the same fashion as the interfacial tension as T increases at fixed L. Our numerical DMRG results agree with this prediction for low temperatures indicating that f_{solv} displays the features of ''classical'' capillary condensation, albeit weakly rounded, in this $d = 2$ model.

For higher temperatures such that $z \equiv L\tau > -10$, the solvation force changes its behavior significantly. As z increases, the jump of f_{solv} gradually transforms into a minimum and plots of $L^2 f_{solv}$ versus $y \equiv L|h|^{8/15}$, obtained for different L, begin to lie closer to a common curve. At $z = -1.26$, the scaling is very good [see Fig. 2(b)]. We confirmed that the scaling also holds above T_c. Moreover, the shape of the scaling function $W_{++}(y) \equiv W(z_0, y, 20\,000)$ for $z_0 = 0.95$ is similar to that below T_c; the depth of the minimum of the scaling function decreases and its position moves monotonically towards $y = 0$ as z_0 increases. Finally, we checked that for $z_0 \approx 0$, as well as for $z_0 < 0$, $W_{++}(y)$ varies as $\approx -y^{1/2}$ for $y \to 0$; see also Figs. 8 and 9 in Ref. [21] which refer to $z_0 \equiv 0$. This implies, via Eq. (9), that the solvation force is a linear function of h for small h and fixed L. Such a result is, of course, predicted by Eq. (18) for $T < T_c$. That it is valid very close to T_c is more surprising and indicates some residual effect of the metastable bulk (condensing) phase.

B. Total adsorption

We have calculated the total adsorption Γ, defined as

$$\Gamma = \sum_{l=1}^{L} m_l, \tag{23}$$

since this quantity also provides an important signature of the first-order phase transition. Γ exhibits a discontinuous jump at capillary condensation from negative values characteristic of a $(-)$ phase, with wetting films of $+$ spins, to positive values characteristic of a $(+)$ phase condensing between the two surfaces. $m_l \equiv \langle \sigma_l \rangle$ is the magnetization in row l. It is straightforward to show using the approximations given earlier and $\Gamma = -L(\partial f/\partial h)_{L,T,h_1}$, that the jump in adsorption

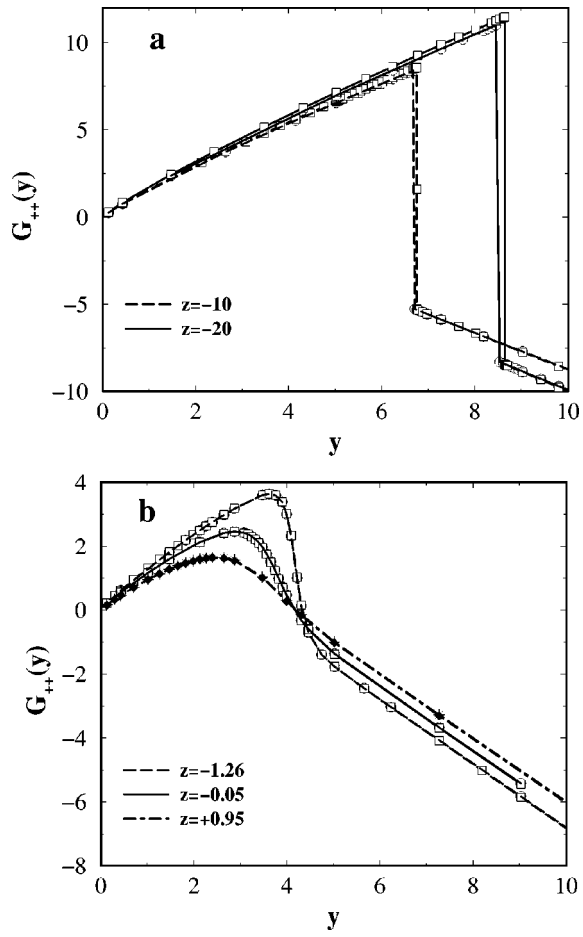

FIG. 3. Dimensionless scaling function of the total adsorption $G_{++}(y)=G(z,y,z)=\Gamma|h|^{7/15}$ plotted as a function of $y=L|h|^{8/15}$ for the same systems and the same choice of scaling variables $x=20\,000$ and various $z=L\tau$ as in Fig. 2. The jumps in (a) occur at the same values of y as those in Fig. 2 and are associated with capillary condensation of the $(+)$ phase (positive adsorption) as y is reduced. In (b) the adsorption exhibits a maximum and scaling is very well obeyed.

$$\Delta\Gamma\equiv\Gamma^{+}-\Gamma^{-}\approx 2m^{*}(T)[L-2l(T,h_{co})], \tag{24}$$

where, as in Eq. (21), $l(T,h_{co})$ is the thickness of a wetting film at capillary coexistence. Plots of Γ versus h for $L=200$ exhibit jumps at low temperature (see Fig. 2 of Ref. [22]) which are consistent with this simple formula. Here, in Fig. 3, we plot the scaling function of the adsorption $G_{++}(y)$ defined by [21]

$$\Gamma=|h|^{(\beta-\nu)/\Delta}G_{++}(y)\equiv|h|^{(\beta-\nu)/\Delta}G(z,y,20\,000), \tag{25}$$

with $(\beta-\nu)/\Delta=-7/15$ in $d=2$, evaluated at the same fixed value $x=Lh_1^2=20\,000$ and the same values of the scaling variable $z=L\tau$ as for the solvation force. As in Fig. 2, for the two lowest values of z, we find very weakly rounded jumps of $G_{++}(y)$ and significant deviations from scaling. Note that the jumps occur at the same values of y as those in $W_{++}(y)$. Closer to the bulk critical point the scaling becomes excellent—see Fig. 3(b). Note that for $z\approx 0$, $G_{++}(y)$ still exhibits a steep increase as y decreases indicating some residual condensation.

C. Longitudinal correlation length

An important quantity that arises in strip geometry is the longitudinal spin-spin correlation length $\xi_{\|}$, which may be expressed in terms of the ratio of the largest Λ_0 and second largest Λ_1 eigenvalues of the transfer matrix

$$\xi_{\|}^{-1}(L,T,h,h_1)=-\ln[\Lambda_1/\Lambda_0]. \tag{26}$$

In the case of *periodic* boundary conditions, the two largest eigenvalues of the transfer matrix are asymptotically degenerate at pseudocoexistence $h=0$, $T<T_c$, and $\xi_{\|}^{-1}\to 0$ as $L\to\infty$. More generally, one knows that the dominant spin configurations of a system at pseudocoexistence involve successive domains of $(+)$ and $(-)$ magnetization of a characteristic length $\xi_{\|}$ separated by domain walls that reach across the strip and $\xi_{\|}$ is related to the interfacial tension $\sigma(T)$ via

$$\xi_{\|}\sim\exp[L\sigma(T)/k_BT], \tag{27}$$

where we ignore prefactors, i.e. $\xi_{\|}^{-1}$ is exponentially small as $L\to\infty$ [23]. For small $|h|$ (but outside the avoided level crossing region) and large L, the inverse correlation length is given by [33]

$$\xi_{\|}^{-1}=2m^{*}(T)|h|L/k_BT. \tag{28}$$

This formula follows from the fact that for small $|h|$ and large L the so-called ''free-energy levels'' $f_0(h,T;L)\equiv-(k_BT/L)\ln\Lambda_0$ and $f_1\equiv-(k_BT/L)\ln\Lambda_1$ are linear functions of h with slopes given by $-m^{*}\mathrm{sgn}(h)$ and $+m^{*}\mathrm{sgn}(h)$, respectively. Note, that in the limit $L\to\infty$, $f_0(h,T;L)$ reduces to the bulk free energy per site.

Little is known about $\xi_{\|}$ in the present case of broken symmetry, $h_1=h_2>0$. We calculate this quantity for a strip of width $L=200$ as a function of h for a series of temperatures (see Fig. 4). At reduced temperatures, $\tau=-0.1011$, -0.0546, and -0.0505, where the solvation force and the adsorption behave in a way characteristic of capillary condensation, $\xi_{\|}^{-1}$ has a sharp minimum at some $h_{min}(T)<0$ with $\xi_{\|}^{-1}(h_{min})\approx 0$ indicating asymptotic degeneracy of Λ_0 and Λ_1. We identify $h_{min}(T)$ with a point of pseudocoexistence noting that the values of $h_{min}(T)$ lie very close to those where Γ and f_{solv} jump—see Figs. 1 and 2 of Ref. [22]. In the close neighborhood of its minimum, $\xi_{\|}^{-1}$ is symmetric and increases linearly in $|h-h_{min}(T)|$.However, the slope is slightly less than that given by Eq. (28) since the slope of f_1 as a function of h appears to be smaller than $m^{*}(T)$. Outside a rather narrow linear region, the variation of the correlation length with h reflects the asymmetry of our system. For $h>h_{min}$, $\xi_{\|}^{-1}$ continues to increase almost linearly, while for $h<h_{min}$, the increase in $\xi_{\|}^{-1}$ is much slower. As the temperature increases, the minimum of $\xi_{\|}^{-1}$ gradually lifts away from zero and becomes more shallow. Whether these fea-

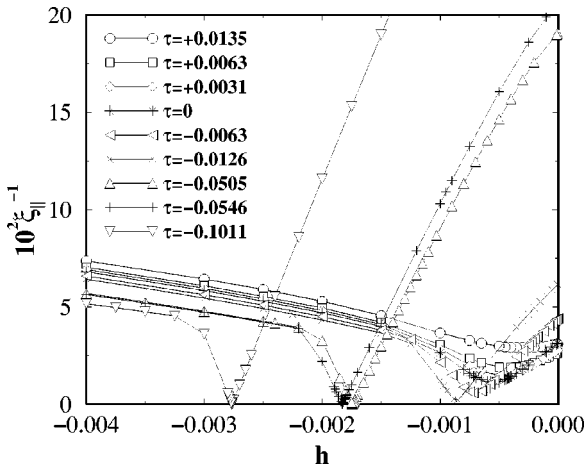

FIG. 4. Inverse longitudinal correlation length (in units of lattice spacing) as a function of the bulk magnetic field h (in units of J) for an Ising strip of fixed width $L=200$, surface fields $h_1=h_2=10$, and several reduced temperatures $\tau\equiv(T-T_c)/T_c$. At the three lowest temperatures, there is a sharp minimum, with $\xi_\parallel^{-1}\approx 0$, which corresponds to pseudocoexistence.

tures may be accounted for by extending the bubble model of Ref. [33] remains to be investigated.

D. Pseudocoexistence line

In Fig. 5, we present the line $h_0(T)$ defined by the maxima of the total free-energy f or, equivalently, by the zeros of the total adsorption Γ, for a strip of fixed width $L=200$. In the same figure, we also plot inflection points of the rounded jump of f_{solv} and the minima, $h_{min}(T)$, of the

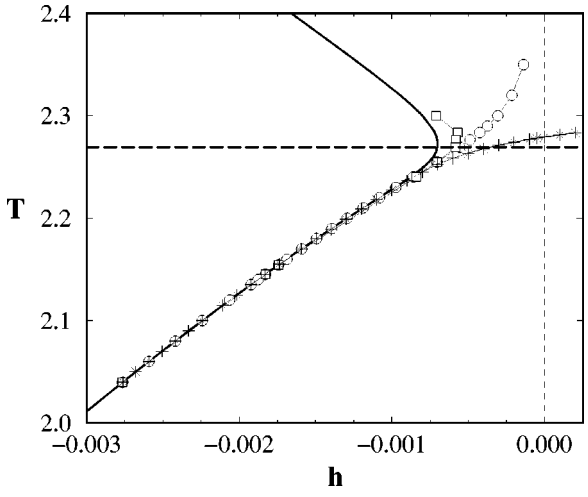

FIG. 5. Maxima $h_0(T)$ of the free energy (or zeros of the adsorption Γ) (solid line), inflection points of f_{solv} (squares), minima of $\xi_\parallel^{-1}$ (circles), and maxima of the specific heat C_H (asterisks) as functions of the bulk magnetic field h (in units of J) calculated at fixed temperature T (in units of J/k_B) for the same system ($L=200$, $h_1=h_2=10$) as in Fig. 4. The bulk critical temperature $T_c\approx 2.269\,185$ ($\tau=0$) is denoted by the horizontal line. Pseudocoexistence between $(-)$ and $(+)$ phases occurs along $h_0(T)$ for $T\lesssim 2.16$ (see text).

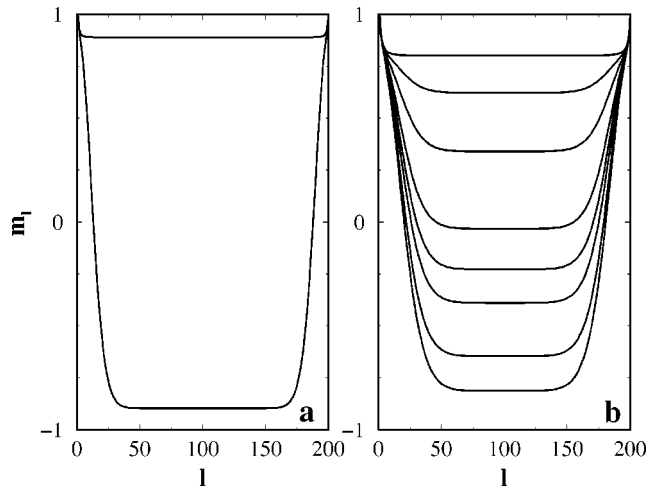

FIG. 6. Variation of the magnetization profile m_l with the temperature at fixed bulk magnetic field h (in units of J): (a) $h=-0.002\,677$ and (b) $h=-0.001\,493$ calculated for the same system as in Figs. 4 and 5, namely, $L=200$, $h_1=h_2=10$. m_l is dimensionless, l is in units of the lattice constant. The top curve in (a) consists of profiles evaluated at $T=2.049\,974$, 2.049 988, 2.049 99, 2.050 002, 2.050 012. The bottom profile corresponds to $T=2.050\,026$. Profiles in (b) correspond to (from top to bottom) $T=2.179\,79$, 2.179 988, 2.179 994, 2.179 998, 2.18, 2.180 002, 2.180 008, 2.1802. (a) corresponds to crossing the pseudocoexistence line while (b) is a ''supercritical'' situation.

inverse correlation length $\xi_\parallel^{-1}$. At low T, these two sets of characteristic points lie on the line $h_0(T)$. For higher T, the curves separate since in the bulk critical region, the behavior of Γ, f_{solv}, and $\xi_\parallel$ reflect different features of criticality. The locus of $h_0(T)$ moves to larger $|h|$ for $T>T_c$, as does the locus of inflection points, whereas $h_{min}(T)$ moves towards $h=0$. Thus, for sufficiently low T, it is natural to identify $h_0(T)$ with the pseudocoexistence line $h_{co}(T)$. Determining the pseudocritical temperature T_{cL} is more difficult since the critical point is not sharp in this quasi-one-dimensional system and we must examine various criteria in order to estimate T_{cL}. The erosion of the jumps in the adsorption and the solvation force takes place for T between 2.155 and 2.160. Another criterion concerns the behavior of the minimum of $\xi_\parallel^{-1}$, which for T between 2.16 and 2.17, lifts away from zero indicating crossover from exponential decay of $\xi_\parallel^{-1}$ with L, characteristic of pseudocoexistence, to a different type of L dependence. The variation of the magnetization profiles with temperature near the line $h_0(T)$ provides a further signature of pseudocoexistence. In Fig. 6, we present data for the evolution of the magnetization profile as a function of temperature T at two fixed values of the bulk field h. For $h=-0.002\,677$, the profile jumps abruptly on crossing the line $h_0(T)$. On the low T side $(+)$ phase, the profile m_l is constant and $\approx m^*(T)$, except very close to the surfaces, while on the high T side $(-)$ phase $m_l\approx -m^*(T)$ in the central region and there are wetting films of $+$ spin at the surfaces. By contrast, for $h=-0.001\,493$, the profiles change continuously as T increases, which implies that the pseudocritical temperature T_{cL} must lie below 2.18. Yet an-

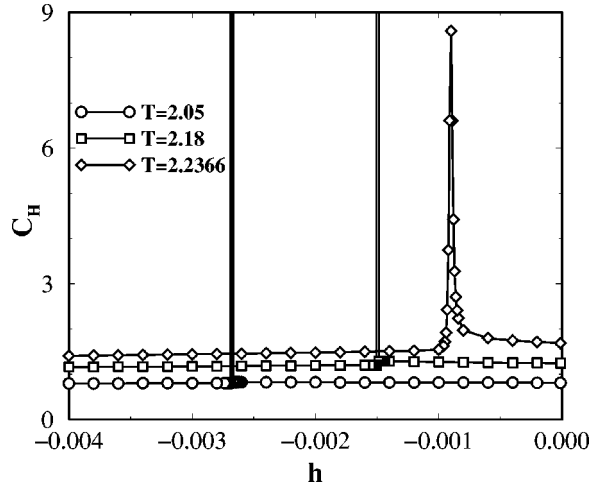

FIG. 7. Specific heat C_H (in units of k_B) calculated for $d=2$ Ising strip of width $L=200$ with surface fields $h_1=h_2=10$ as a function of h (in units of J) at fixed temperatures $T=2.05$, 2.18, 2.2366 (in units of J/k_BT). Note that the maxima which occur for the two lowest temperatures are off the scale of the present figure.

other indicator of pseudocoexistence is the specific heat, which we discuss in the next subsection.

E. Specific heat

Second derivatives of free energies (response functions) usually provide key information about the nature of phase transitions. Although the behavior of the susceptibility χ at a capillary condensation transition in $d=2$ Ising systems has been studied in Monte Carlo simulations [34], the specific heat $C_H(L,T,h,h_1)\equiv -T(\partial^2 f/\partial T^2)_{L,h,h_1}$ does not seem to have been investigated [35]. In the bulk Ising system, the specific heat has quite different behavior from the susceptibility as the phase boundary is crossed by changing h at fixed $T<T_c$: χ exhibits a delta-function singularity at $h=0$, whereas Ising symmetry ensures that C_H shows no jump (no latent heat).

For the case of Ising strips in $d=2$ subject to surface fields $h_1=h_2>0$, we expect the singularity in χ to occur at capillary condensation, i.e., it should occur on the line $h_{co}(T)<0$ and be weakly (exponentially small in L) rounded. What do we expect for C_H near the (pseudo) transition?

If the broken symmetry, arising from the surface fields, modifies the phase diagram to that in Fig. 1(a), so that $dh_{co}/dT>0$, the latent heat should manifest itself either by varying h at fixed T or by varying T at fixed h. In other words, there is ''field mixing'' and C_H and χ should acquire the same type of weakly rounded singularity. We have chosen to analyze C_H as this quantity is readily calculable from the total free energy obtained in DMRG.

Figure 7 shows C_H versus h for $L=200$ and three temperatures below T_c: $T=2.05;2.18;2.2366$. For each temperature, there is a pronounced maximum at some $h_{max}(T)<0$, which shifts towards $h=0$ as the temperature increases. At $T=2.05$, the maximum is extremely high and extremely narrow in h, whereas for $T=2.18$, its height is reduced and it is more rounded, although this is not obvious on the scale of the figure. For $T=2.2366$, the rounding is clearly apparent. The locus of $h_{max}(T)$ is plotted in Fig. 5 (asterisks) and lies on top of $h_0(T)$ (maxima of free energy) until rather high temperatures $T\approx 2.21$ when small deviations occur. On approaching T_c, the height of the maximum in C_H reduces rapidly and it moves quickly towards $h=0$. In zero bulk field, C_H takes its maximum value above T_c at $T=2.2793$, corresponding to reduced temperature $\tau=0.0045$. We should note that the minimum of f_{solv} at $h=0$ is located at a slightly higher temperature $T=2.2835$ or $\tau=0.006\,31$ and that $\xi_{\|}^{-1}$ at $h=0$ has its minimum at $T=2.287$, very close to that of f_{solv}.

In Fig. 8, we plot C_H as a function of the temperature for the same two values of the bulk field h at which the magnetization profiles were calculated in Fig. 6, namely $h=-0.002\,677$ and $h=-0.001\,493$. For both cases, there is a pronounced symmetric maximum. This is very sharp for h

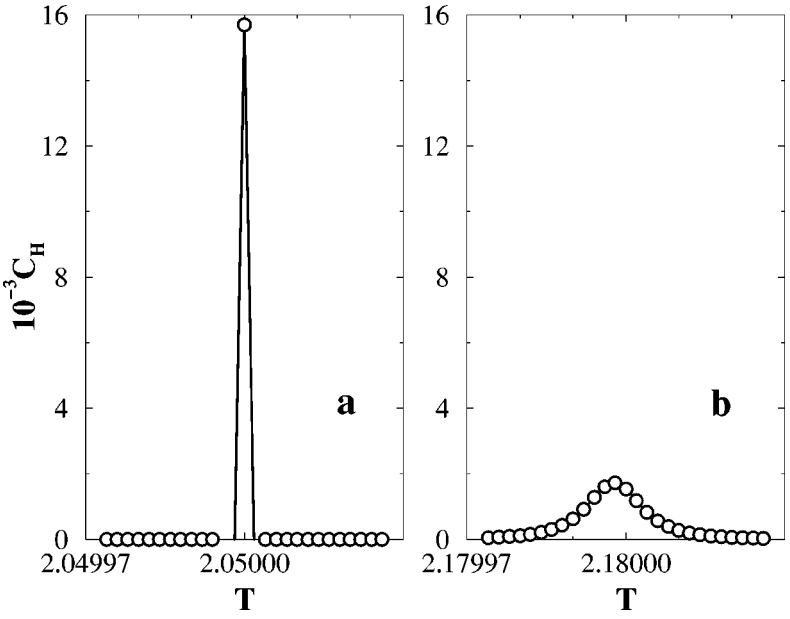

FIG. 8. Specific heat C_H (in units of k_B) calculated for the same system as in Fig. 7 but now as a function of temperature T (in units of J/k_B) at fixed bulk field (a) $h=-0.002\,677$ and (b) $h=-0.001\,4935$. Note the very fine temperature scale.

$=-0.002\,677$ [Fig. 8(a)] whereas for $h=-0.001\,493$, it is much reduced in height and is significantly broadened [Fig. 8(b)]. Such behavior is consistent with the temperature variation of the profiles. The smooth variation of C_H in case (b) reflects the smooth variation of the profiles shown in Fig. 6(b) and confirms that $T=2.18$ is ''supercritical.''

The variation of C_H with h is less symmetric than the variation with T. Close examination of Fig. 7 shows that for each temperature, C_H increases with increasing h up to the ''transition'' and decreases thereafter. We attempt to understand this feature of the results by considering the simple theory for the free energies of the two ''phases'' that we used to describe capillary condensation in Sec. III A. From the approximation (13), we may obtain the specific heat in the $(-)$ and $(+)$ phases. Expanding the bulk free energy [see Eq. (16)] to first order in h we find

$$C_H^- \approx C_{Hb}^-(T,0) - (Th)\frac{d^2m^*(T)}{dT^2} - (2T/L)\frac{\partial^2 f_w^-}{\partial T^2} \quad (29)$$

and

$$C_H^+ \approx C_{Hb}^+(T,0) + (Th)\frac{d^2m^*(T)}{dT^2} - (2T/L)\frac{\partial^2 f_w^+}{\partial T^2}, \quad (30)$$

where $C_{Hb}^-(T,0)=C_{Hb}^+(T,0)\equiv C_{Hb}(T)$ is the bulk specific heat at coexistence $h=0$. If we also expand the surface excess free energy $f_w^{\pm}$ as in Eq. (19), it follows that

$$C_H^- \approx C_{Hb}(T) - Th\frac{d^2m^*(T)}{dT^2}\left(1-\frac{4l(T,h_{co})}{L}\right) + \frac{4Th}{L}m^*(T)\frac{\partial^2 l(T,h_{co})}{\partial T^2} - \frac{2T}{L}\frac{\partial^2 \sigma_w^-(T,h_1)}{\partial T^2} \quad (31)$$

and

$$C_H^+ \approx C_{Hb}(T) + (Th)\frac{d^2m^*(T)}{dT^2} - (2T/L)\frac{\partial^2 \sigma_w^+(T,h_1)}{\partial T^2}, \quad (32)$$

where we have assumed, as previously, that $m_s^+ \approx 0$ and $m_s^- \approx 2l(T,h_{co})m^*(T)$, with $l(T,h_{co})$ the thickness of the wetting film near capillary condensation. For large L, we expect the bulk terms to dominate and noting that $d^2m^*(T)/dT^2<0$, it follows that C_H should increase linearly with h as $h\to h_{co}^-(T)$ and decrease linearly for h slightly larger than $h_{co}(T)$, as is found in Fig. 7. The difference in heat capacity between the two ''phases'' should be given by $C_H^+ - C_H^- \approx 2Th_{co}(T)(d^2m^*(T)/dT^2)$, where, once again, we have ignored surface contributions.

Of course, this simple treatment was designed for true capillary condensation as would occur in a three-dimensional Ising system. It does not describe the weakly rounded singularity that occurs in the present two-dimensional system. Nevertheless, it does seem to account for the variation of C_H with h that is observed slightly away from $h_{co}(T)$.

To complete this section we note that the symmetry breaking associated with the surface fields leads to a nonzero latent heat at the condensation transition, i.e., the entropy difference between the $(+)$ and $(-)$ phases is nonzero—as one would glean from the magnetization profiles in Fig. 6(a). The latent heat is proportional to the slope of the coexistence curve, which may be estimated from the Kelvin equation (20). It should be inversely proportional to L, the width of the strip.

IV. DMRG RESULTS FOR SURFACE FIELDS $h_1=h_2=0$

In this section, we consider the Ising strip with free boundaries, i.e., the surface fields $h_1=h_2=0$. This is the case whose phase diagram is described in Fig. 1(b). Now the Ising symmetry $h\Leftrightarrow -h$ is preserved and (pseudo) coexistence occurs along $h=0$:$h_{co}(T)=0$. Crossing this line gives rise to a jump in the total adsorption from $\Gamma \approx -Lm^*(T)$ for $h<0$, $(-)$ phase, to $\Gamma \approx +Lm^*(T)$ for $h>0$, $(+)$ phase. However, unlike the case of nonzero surface fields, there is no jump in the solvation force and no singularity in the heat capacity. The susceptibility χ does exhibit a weakly rounded singularity.

If we restrict consideration to bulk field $h=0$, it is possible to obtain *exact* transfer matrix solutions and we summarize some of the main results here. These provide valuable benchmark data against which DMRG may be tested. We then apply the DMRG for $h\neq 0$, where exact solutions are not available.

The solvation force f_{solv} was analyzed by Evans and Stecki [19]. They showed that the scaling function W, defined by Eq. (9) has the property, for $d=2$,

$$W_{00}(-L\tau,0,0) = W_{++}(L\tau,0,\infty), \quad (33)$$

where subscripts 00 refer to $h_1=h_2=0$ and $++$ to $h_1=h_2=\infty$. This implies that for free boundaries, the solvation force evaluated at $h=0$, in the scaling limit, has a minimum at $z\equiv L\tau=-1.2642$ [19]. In Fig. 9(a), we plot f_{solv} as a function of T for $L=200$, $h=0$ and $h_1=h_2=0$ obtained using the formulas given in Ref. [19] and, for comparison, results obtained by the DMRG method. The agreement is excellent.

Exact expressions for the specific heat C_H and its scaling function were derived by Au-Yang and Fisher [36]. C_H evaluated at $h=0$ has its maximum at $z\equiv L\tau=-0.8929$. In Fig. 9(b), we present the DMRG results for C_H obtained for $L=200$, c.f. Fig. 9(a). As one can ascertain from the inset, the maximum obtained from the DMRG is at the same value as that given by the exact result (relative error 10^{-5} or less). This gives us confidence in the accuracy of the DMRG technique and in our numerical methods for obtaining C_H.

The behavior of $\xi_{\parallel}^{-1}$ may also be determined from the exact diagonalization of the transfer matrix [37]. For large L and low temperatures so that $L\sigma(T)/k_BT \gg 1$, $\xi_{\parallel}^{-1}$ is exponentially small in L

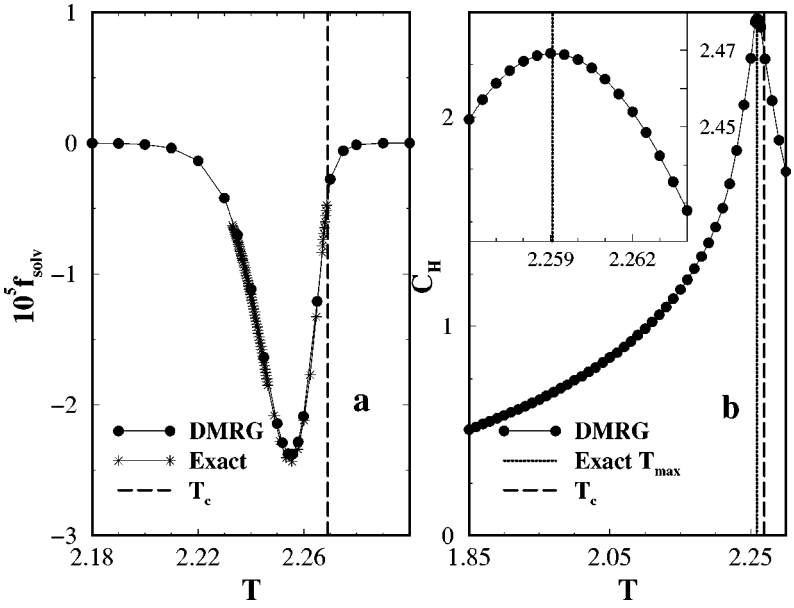

FIG. 9. (a) Solvation force (in units of J) and (b) specific heat C_H (in units of k_B) as a function of the temperature T (in units of J/k_B) at vanishing bulk field $h=0$ for the $d=2$ Ising strip of width $L=200$ with free boundary conditions: $h_1=h_2=0$. In (a) the circles denote the DMRG results and asterisks the results from the exact diagonalization of the transfer matrix. In (b) the circles denote the DMRG results and the vertical dotted line the maximum of C_H given by an exact calculation: $T_{max}=2.25906$. The inset shows, on an expanded scale, that the DMRG results have their maximum at the same position.

$$\xi_{\parallel}^{-1} \approx 2(\sinh[\sigma(T)/k_BT]/\sinh 2K)\exp[-L\sigma(T)/k_BT]. \tag{34}$$

As $T \to T_c^-$ the surface tension, given by Eq. (5), vanishes as $\sigma(T)/k_BT \approx -4K_c\tau \to 0$, where $\sinh 2K_c = 1$, i.e., $K_c \approx 0.440\,68$, and for $z \approx 1$, Eq. (34) is no longer valid. In the regime $z \equiv L\tau \sim -1/4K_c$ the form of $\xi_{\parallel}^{-1}$ crosses over to [37]

$$\xi_{\parallel}^{-1} \approx \sigma(T)/k_BT + \pi/2L \approx -4K_c\tau + \pi/2L. \tag{35}$$

Figures 10 and 11 show DMRG results for f_{solv} and C_H, respectively, as a function of h at several values of T for $L=200$. Both functions are symmetric in h, so we show results for $h \geqslant 0$ only. For the two lowest temperatures, f_{solv} is almost zero and nearly constant in h. As T increases $f_{solv}(h=0)$ becomes more attractive and f_{solv} increases monotonically with h. For higher temperatures, f_{solv} develops a sharp minimum at $h>0$; this decreases in depth and shifts to larger values of h as T increases towards T_c. This trend persists for $T>T_c$; for $\tau=0.0063$, $f_{solv}(h=0)$ is almost zero, but there is still significant attraction for $h>0$ with a broad minimum near $h=2.4\times10^{-4}$.

The results for the specific heat in Fig. 11 exhibit equivalent features. At low temperatures, C_H decreases monotonically with h, whereas for higher temperatures, a maximum develops at $h>0$. At $\tau=-0.0045$, where $C_H(h=0)$ takes its maximum value, the maximum occurs near $h=4\times10^{-5}$. As

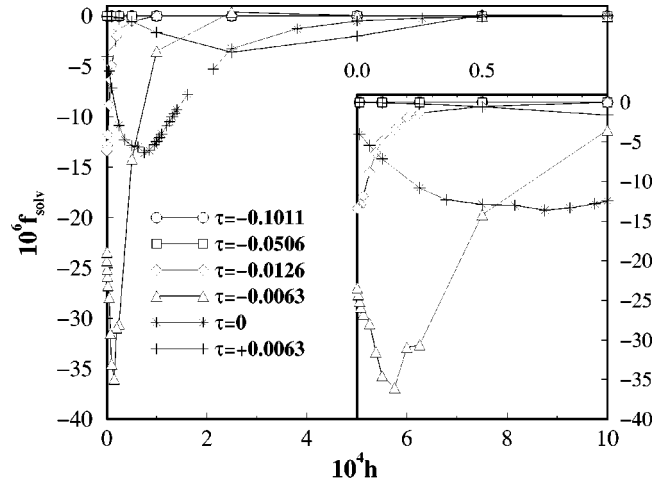

FIG. 10. Solvation force f_{solv} (in units of J) as a function of the bulk field h (in units of J) at several reduced temperatures $\tau \equiv (T-T_c)/T_c$ calculated using the DMRG method for the $d=2$ Ising strip of width $L=200$ with free boundary conditions: $h_1=h_2=0$. The inset shows the results on an expanded horizontal scale near $h=0$. Note that the minimum value of $f_{solv}(h=0)$ occurs at $\tau=-0.0063$ (triangles).

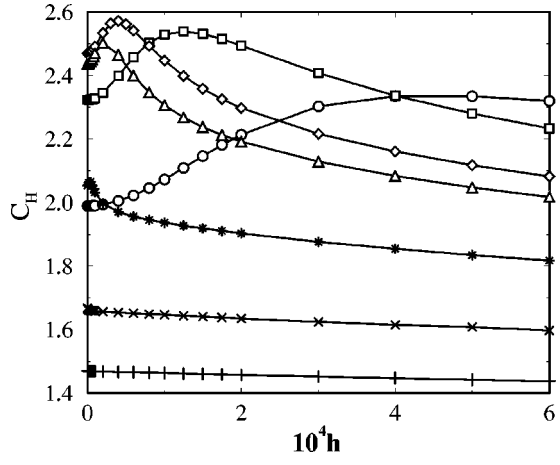

FIG. 11. Specific heat C_H (in units of k_B) as a function of the bulk field h (in units of J) at several temperatures close to the critical temperature T_c: $\tau \equiv (T-T_c)/T_c = -0.0305$ (pluses), -0.0217 (crosses), -0.0126 (asterisks), -0.0063 (triangles), -0.0045 (diamonds), 0 (squares), 0.0063 (circles), calculated using the DMRG method for the $d=2$ Ising strip of width $L=200$ with free boundary conditions: $h_1=h_2=0$. Note that the maximum value of $C_H(h=0)$ occurs at $\tau=-0.0045$ (diamonds).

T is increased further, $C_H(h=0)$ decreases rapidly, and the maximum shifts to larger values of h.

The appearance of two symmetric minima in f_{solv}, at $h_{min}>0$ and $-h_{min}$, could have been anticipated on the basis of our previous DMRG results for $T=T_c(\tau=0)$ where the scaling function $W(0,y,0)$, with $y\equiv L|h|^{8/15}$, was determined [21]. That scaling function has its minimum near $y=1.12$, which corresponds to $L\sim 2.9\xi_b$, where ξ_b is the (T and h dependent) bulk correlation length. Our present results show the evolution of the symmetric minima as a function of temperature. It is likely that the position of the minimum h_{min} is determined by a criterion such as $L\sim\xi_b$ for all temperatures in the neighborhood of T_c, but we have not investigated this in detail. We would expect the two symmetric maxima in C_H to be determined by a similar criterion but with a different numerical prefactor.

Finally, we remark that the temperatures at which the specific heat $C_H(h=0)$ has its maximum and the solvation force $f_{solv}(h=0)$ has its minimum both lie above what we might identify as a pseudocritical temperature. The latter may be estimated very crudely by considering the small h dependence of the adsorption and of $\xi_{\|}^{-1}$ and we find that for $L=200$, $\tau=-0.0126$, or $T=2.23$ is already ''supercritical,'' i.e., there has been crossover into a regime different from pseudocoexistence.

V. DISCUSSION

In this paper, we have employed the DMRG technique to investigate various properties of two-dimensional Ising strips of width L subject to identical surface fields. We have considered temperatures T above and below the bulk critical temperature T_c and a range of bulk fields h. In the case of nonvanishing surface fields, $h_1=h_2>0$, the preferential adsorption of $(+)$ spins at each wall leads to a shift of the bulk phase boundary to $h<0$. This phenomenon of (pseudo) capillary condensation has a profound influence on many properties of the Ising strip, not just at low temperatures where the (weakly rounded) condensation transition takes place, but also for T above the pseudocapillary critical temperature T_{cL}, i.e., for T near T_c. The most pronounced features in the solvation force f_{solv}, adsorption Γ, inverse longitudinal correlation length $\xi_{\|}^{-1}$, and specific heat C_H occur along the continuation to higher T of the pseudocoexistence line—see Fig. 5. There is strong variation with T and h. For example, for $L=200$ and a reduced temperature $\tau=-0.0126$, which lies above $T_{c,L}$, the minimum value of the solvation force is about 300 times the Casimir value, corresponding to $h=0,\tau=0$.

We confirmed that finite-size scaling is very well obeyed for f_{solv} and Γ (see Figs. 2 and 3) provided one avoids the low-temperature, condensation transition. Scaling is equally well obeyed for $\xi_{\|}^{-1}$, although we do not display its scaling plots here.

The effect of the surface fields $h_1=h_2>0$ is to break the $h\Leftrightarrow -h$ Ising symmetry so that field mixing occurs. We find that C_H exhibits a very weakly rounded singularity on crossing the pseudocoexistence line either by increasing h at fixed T or by increasing T at fixed h—see Figs. 7 and 8. For higher temperatures, C_H exhibits a very pronounced maximum, which lies close to the extrema calculated for other quantities until T is very close to T_c when deviations occur—see Fig. 5.

We also carried out calculations for the case of free boundaries $h_1=h_2=0$. Since exact results are available for the particular case $h=0$, this allowed us to confirm the accuracy of the DMRG—see Fig. 9. For free boundaries Ising symmetry is not broken and the various properties exhibit a rather different variation with T and h from these obtained with nonzero surface fields. For temperatures slightly below T_c, f_{solv} develops two sharp minima symmetric in h (Fig. 10), i.e., the solvation force is more attractive in nonzero field. Similarly, C_H develops two symmetric maxima—see Fig. 11.

Our present results are for $d=2$. We may speculate as to what might occur in the $d=3$ Ising film with $h_1=h_2>0$. Now there is true capillary coexistence along a line $h_{co}(T)$ ending in a true capillary critical point at (h_{cL},T_{cL}). f_{solv}, Γ, and C_H should exhibit similar features to those found in $d=2$. Below T_{cL}, f_{solv} will exhibit a discontinuous jump: $\Delta f_{solv}\sim -2\sigma(T)/L$ [see Eq. (22)] accompanied by a jump: $\Delta\Gamma\sim 2Lm^*(T)$ in the total adsorption [see Eq. (24)]. On the critical isotherm $T=T_{cL}$, the jumps are eroded with $\Delta\Gamma\sim(h_{cL}-h)^{1/\delta}$, as $h\to h_{cL}^-$, where $\delta=15$ corresponds to the $d=2$ Ising exponent. For temperatures above T_{cL}, f_{solv} and Γ should exhibit scaling functions similar to those shown here in Figs. 2 and 3 but with the appropriate scaling variables $y=L|h|^{\nu/\Delta}$ and $z=L\tau^{\nu}$ now determined by the $d=3$ bulk critical exponents ν and Δ. Moreover, for $T<T_c$ and small $|h|$, f_{solv} should still be given by Eq. (18), i.e., it should increase linearly with h. Since the gradient is $\sim 2m^*(T)$, it should vanish as $(-\tau)^{\beta}$ with $\beta\approx 0.325$ in $d=3$. Such behavior is an important signature of residual condensation and is found in explicit mean-field results [38] for a Landau (square-gradient) theory, where $\beta=1/2$.

For the $d=3$ film with free boundaries, the solvation force and specific heat should exhibit similar behavior to that shown in $d=2$, i.e., similar to in Figs 9–11. The extrema may be less pronounced, and will lie at somewhat different positions in the phase diagram since the scaling functions will be different. Nevertheless, we expect the overall T and h variation to be similar.

Finally, we return to the implications of our results for real confined fluids. A pure fluid confined by strongly adsorbing walls (favoring liquid) should exhibit the same features as the $d=3$ Ising film with $h_1=h_2\gg 0$. Thus, capillary condensation will manifest itself in the same way for fluids as for Ising magnets and this can be analyzed in the same fashion provided one replaces $2m^*(T)$ by $\rho_l-\rho_g$, the difference in coexisting densities of the bulk liquid and gas phases at temperature T, and h by $\mu-\mu_{sat}(T)$, the chemical-potential difference. The critical scaling functions should also be equivalent, although one must be cautious about the choice of scaling variables since field mixing already occurs for a bulk liquid. For a binary liquid mixture that undergoes bulk liquid-liquid phase separation, there is also the analogue of capillary condensation [2,5,12]. Depending on which spe-

cies the walls favor, phase separation may be shifted to lower or higher compositions than in bulk. In such mixtures, we would also expect to find a strongly attractive solvation force for temperatures between T_{cL} and T_c and for compositions lying on the condensation side of the bulk critical composition. Our study has shown that the behavior of *near* critical confined fluids is very rich; it is not just the behavior exactly at the bulk critical point (the critical Casimir effect) which is of interest. Thus, experiments that aim to measure the Casimir force, e.g., by atomic force microscopy or surface force apparatus, should also investigate the h and τ dependence of f_{solv}.

Similar remarks apply to measurements of other thermodynamic quantities [39]. It is the scaling functions that provide the most information—the same point has been made by Krech and Krech and Dietrich [8,15,16].

As a last remark, we note that the existence of a long-ranged, strongly attractive solvation force between two macroscopic walls has important repercussions for the effective force between two large (colloidal) particles immersed in a near-critical fluid or binary liquid mixture. If one can ascertain where f_{solv} is most attractive, this should help determine where aggregation or flocculation of a suspension of the large particles is potentially the strongest. There is a growing literature on this topic [13,18,40].

ACKNOWLEDGMENTS

We are grateful to K. Binder for valuable correspondence and to J. M. J. van Leeuwen, A. Ciach, A. O. Parry, and P. J. Upton for helpful comments and discussions. This work was partially funded by KBN Grant Nos. 2P03B10616 and 3T09A07316 and by Polish Academy of Sciences–Royal Society Travel Grants.

[1] R. Evans, J. Phys.: Condens. Matter **2**, 8989 (1990), and references therein.
[2] L.D. Gelb, K.E. Gubbins, R. Radhakrishnan, and M. Śliwińska-Bartkowiak, Rep. Prog. Phys. **62**, 1573 (1999).
[3] M.N. Barber, in *Phase Transitions and Critical Phenomena*, edited by C. Domb and J.L. Lebowitz (Academic, London, 1983), Vol. 8, p. 145.
[4] V. Privman, in *Finite Size Scaling and Numerical Simulation of Statistical Systems*, edited by V. Privman (World Scientific, Singapore, 1990), p. 1.
[5] M.E. Fisher and H. Nakanishi, J. Chem. Phys. **75**, 5857 (1981); H. Nakanishi and M.E. Fisher, *ibid.* **78**, 3279 (1983).
[6] For a general review of critical behavior at surfaces, see K. Binder, in *Phase Transitions and Critical Phenomena*, edited by C. Domb and J.L. Lebowitz (Academic, London, 1983), Vol. 8, p. 1.
[7] H.W. Diehl, in *Phase Transitions and Critical Phenomena*, edited by C. Domb and J.L. Lebowitz (Academic, London, 1986), Vol. 10, p. 75; H.W. Diehl, Int. J. Mod. Phys. B **11**, 3503 (1997).
[8] M. Krech, *The Casimir Effect in Critical System* (World Scientific, Singapore, 1994), and references therein; J. Phys.: Condens. Matter **11**, R391 (1999).
[9] M.E. Fisher and P.-G. de Gennes, C. R. Seances Acad. Sci., Ser. B **287**, 207 (1978).
[10] H.B.G. Casimir, Proc. K. Ned. Akad. Wet. **51**, 793 (1948).
[11] R. Evans, U. Marini Bettolo Marconi, and P. Tarazona, J. Chem. Phys. **84**, 2376 (1986).
[12] R. Evans and U. Marini Bettolo Marconi, J. Chem. Phys. **86**, 7138 (1987).
[13] B.M. Law, Prog. Surf. Sci. **66**, 159 (2001).
[14] A. Mukhopadhyay and B.M. Law, Phys. Rev. Lett. **83**, 772 (1999); R. Garcia and M.H.W. Chan, *ibid.* **83**, 1187 (1999).
[15] M. Krech and S. Dietrich, Phys. Rev. A **46**, 1886 (1992); **46**, 1922 (1992).
[16] M. Krech, Phys. Rev. E **56**, 1642 (1997).
[17] Z. Borjan and P.J. Upton, Phys. Rev. Lett. **81**, 4911 (1998); Z. Borjan, Ph.D thesis, University of Bristol, 1999.
[18] A. Hanke, F. Schlesener, E. Eisenriegler, and S. Dietrich, Phys. Rev. Lett. **81**, 1885 (1998).
[19] R. Evans and J. Stecki, Phys. Rev. B **49**, 8842 (1993).
[20] T. Nishino, J. Phys. Soc. Jpn. **64**, 3598 (1995).
[21] A. Drzewiński, A. Maciołek, and A. Ciach, Phys. Rev. E **61**, 5009 (2000).
[22] A. Drzewiński, A. Maciołek, and R. Evans, Phys. Rev. Lett. **85**, 3079 (2000).
[23] V. Privman and M.E. Fisher, J. Stat. Phys. **33**, 385 (1983), and references therein.
[24] K. Binder, Rep. Prog. Phys. **60**, 487 (1997).
[25] E.V. Albano, K. Binder, and W. Paul, J. Phys. A **30**, 3285 (1997).
[26] E. Carlon, A. Drzewiński, and J. Rogiers, Phys. Rev. B **58**, 5070 (1998).
[27] L. Onsager, Phys. Rev. **65**, 117 (1944).
[28] S.R. White, Phys. Rev. Lett. **69**, 2863 (1992).
[29] See, e.g., *Lecture Notes in Physics*, edited by I. Peschel, X. Wang, M. Kaulke, and K. Hallberg (Springer, Berlin, 1999), Vol. 528.
[30] H.W. Blöte, J.L. Cardy, and M.P. Nightingale, Phys. Rev. Lett. **56**, 742 (1986).
[31] R. Bulirsch and J. Stoer, Numer. Math. **6**, 413 (1964); M. Henkel and G. Schütz, J. Phys. A **21**, 2617 (1988).
[32] A.O. Parry and R. Evans, J. Phys. A **25**, 275 (1992). The validity of the leading, $O(1/L)$ Kelvin result was confirmed by DMRG in Ref. [26] and by Monte Carlo in Ref. [25]. Establishing the precise form of the corrections requires very large values of L so that thick wetting films may develop at capillary coexistence.
[33] D.B. Abraham, A.O. Parry, and P.J. Upton, Phys. Rev. E **51**, 5261 (1995).
[34] E.V. Albano, K. Binder, D.W. Heermann, and W. Paul, J. Chem. Phys. **91**, 3700 (1989).
[35] Both χ and C_H were investigated in Monte Carlo simulations of capillary condensation in the $d=3$ Ising system. Both quantities exhibit singularities rounded by the finite area of the simulation. K. Binder and D.P. Landau, J. Chem. Phys. **96**, 1444 (1992).

[36] H. Au-Yang and M.E. Fisher, Phys. Rev. B **11**, 3469 (1975).
[37] D.B. Abraham, Stud. Appl. Math. **50**, 71 (1971).
[38] F. Schlesener (private communication).
[39] Competing bulk and surface fields also give rise to interesting behavior of the total adsorption Γ as a function of temperature at fixed, small $h<0$. As $\tau\rightarrow 0^{+}$, Γ first increases (critical adsorption) but then decreases rapidly to negative values very close to T_c. This phenomenon is termed critical depletion; see A. Maciołek, A. Ciach, and R. Evans, J. Chem. Phys. **108**, 9765 (1998).
[40] For an instructive summary of experimental and theoretical work see, T. Bieker and S. Dietrich, Physica A **252**, 85 (1998); C. Bauer, T. Bieker, and S. Dietrich, Phys. Rev. E **62**, 5324 (2000).